Drosophila Toll links systemic immunity to long-term intestinal function.

Magda L. Atilano[1,2], Marcus Glittenberg[2], Shivohum Bahuguna, Lihui Wang and Petros Ligoxygakis

Laboratory of Cell Biology, Development and Genetics, Department of Biochemistry, University of Oxford, South Parks Rd OX1 3QU Oxford UK.

[1]Present address: Institute for Healthy Aging, University College London, Gower Street WC1E 6BT, London UK.

[2]These authors contributed equally to this work

Lead Contact and corresponding author: petros.ligoxygakis@bioch.ox.ac.uk

Abstract: The intestine is an organ where immune and metabolic functions are co-ordinated with tissue renewal via progenitor somatic stem cells (PSSCs). How this is achieved is still unclear. We report that in *Drosophila*, a generalised infection increased PSSC numbers. This was mimicked by expressing a constitutive form of the immune receptor Toll in PSSCs and blocked when Toll was silenced via RNAi. Without infection, absence of bacterial recognition and downstream Toll signalling resulted in a short lifespan and an age-dependent decrease of PSSCs and gut microbiota. The latter implied a metabolic environment incompatible with the presence of bacteria. Indeed, infection or constitutive Toll signalling in PSSCs triggered 4E-BP transcription in enterocytes, while loss of signalling reduced it. 4E-BP controlled fat levels and sustained the microbiota suggesting that Toll-dependent regulation of 4E-BP was important for long-term gut function. Therefore, the Toll pathway is crucial for responses to both infection and microbiota.

To Thanasis Loukeris *in memoriam*

Introduction: Innate immunity is the first-line host defence conserved in all metazoans and plants (reviewed in Ronald and Beutler, 2010). In this context, Toll-like receptor (TLR) signalling is one of the most important mechanisms by which the innate immune system senses the invasion of pathogenic microorganisms in both mammals and Drosophila. Unlike its mammalian counterparts however, the fruit fly Toll is activated by an endogenous cytokine-like ligand, the Nerve Growth Factor homologue, Spz (Weber et al, 2003). Spz is processed to its active form by the Spz-Processing Enzyme (SPE) (Jiang et al, 2006). Two serine protease cascades converge on SPE: one triggered by bacterial or fungal serine proteases and a second activated by host receptors that recognise bacterial or fungal cell wall. Prominent among these host receptors is the Peptidoglycan Recognition Protein-SA or PGRP-SA (Michel et al, 2001), which is considered to preferentially bind to Lys-type Peptidoglycan from Gram-positive bacteria (Chang et al, 2004). When the recognition signal reaches the cell surface, it is communicated downstream via the Toll receptor and a membrane-bound receptor-adaptor complex including dMyd88, Tube (as an IRAK4 functional equivalent) and the Pelle kinase (as an IRAK1 functional homologue) (Marek and Kagan 2012). Transduction of the signal culminates in the phosphorylation of the IκB homologue, Cactus (Daigneault et al, 2013). This modification requires the fly βTrCP protein Slimb (Daigneault et al, 2013) and targets Cactus for degradation, leaving the NF-κB homologue DIF to move to the nucleus and regulate hundreds of target genes including a battery of powerful antimicrobial peptides (AMPs) (de Gregorio et al, 2002).

Similar to mammals, the high capacity of intestinal epithelial regeneration in *Drosophila* depends on intestinal stem cells (ISCs). These multipotent ISCs, which are distributed along the basement membrane of the posterior midgut have a simple pattern of division (Ohlstein and Spradling 2006; Ohlstein and Spradling 2007, reviewed in Lemaitre and Miguel- Aliaga, 2013). An ISC divides to produce itself and an enteroblast (EB), which will undergo terminal differentiation into an enterocyte (EC) or an enteroendocrine cell (EE). Progenitor cells (ISCs and EBs) express a transcription factor called Escargot (esg) (Ohlstein and Spradling 2006; Ohlstein and Spradling 2007;

Amcheslavsky et al 2009). Thus, expression of *esg* is often used as a surrogate marker for studying both ISCs and EBs in the anterior midgut. Previous studies have shown that direct local damage to the gut by oxidative stress, toxins or ingestion of bacteria leads to EC apoptosis, stimulating ISCs to proliferate and replenish EC numbers (Amcheslavsky et al 2009; Buchon et al, 2009). In this context, intestinal microbiota impacted on the rate of ISC proliferation by stimulating them to keep a higher "baseline" of epithelial turnover (Buchon et al, 2009). However, less is known about what happens after systemic infection. Septic injury with the Gram-negative bacterium *Erwinia carotovora carotovora-15 (Ecc-15)* promotes ISC proliferation through cytokine signalling mediated by blood cells (Chakrabarti *et al*, 2016). In addition, sterile wounding also causes EC apoptosis and triggers ISC proliferation (Takeishi et al, 2013).

The intestine has also a metabolic role and this depending on the context is coordinated by insulin, FOXO and TOR (reviewed in Miguel-Aliaga *et al,* 2018). One of the downstream components of this signalling network is the translational inhibitor 4E-BP (Miron et al, 2003). It has been hypothesised that the control of 4E-BP activity in flies could provide a means to control fat metabolism during stress conditions (Teleman et al, 2005). In adults, 4E-BP is important for infections that activate the Toll pathway, since 4E-BP mutant flies are highly susceptible to fungal and Gram-positive bacterial infections (Bernal and Kimbrell 2000). In larvae, FOXO induces 4E-BP activation following *Ecc-15* oral infection or starvation stress, which tips the balance towards translation of cap independent transcripts including AMPs (Vasuvedan *et al*, 2017). Thus, 4E-BP may provide the link between systemic Toll activation and metabolic control.

After the discovery of intestinal T-cells expressing TLRs, we know that the immune system can discriminate between and regulate appropriate responses towards, non-infectious non-self (e.g. gut microbiota) vs. infectious non-self (reviewed in Kubinak and Round 2012). However, it is less clear how immune response signals from a systemic infection will be integrated at the intestine level by ISCs and ECs with the aim of maintaining tissue integrity and normal gut microbiota. In the present

work, we investigated how systemic infection triggering Drosophila Toll/TLR signalling may be linked to long-term intestinal homeostasis.

Results and discussion: To trace intestinal progenitor cells (ISCs and EBs) we used the GAL4/GAL80^{ts}/UAS system (Suster et al, 2004). The driver for GAL4 expression was the *esg* gene promoter. Normally, GAL80 is an inhibitor of GAL4 but the temperature sensitive allele used was able to do this only at the permissive temperature (18^{o}C) and not at the restrictive temperature (30^{o}C). In all the experiments described in this work, developing flies were cultured at 18^{o}C and on eclosion emerging adults were shifted to 30^{o}C. When 20-day old adults expressing GFP under the *esg* promoter in the anterior midgut (Fig. 1A) were injected in the thorax with the opportunistic fungal pathogen *Candida albicans* (*C. albicans*), we observed a statistically significant increase of GFP-positive cells 36h post-infection (Fig. 1B). This result indicated that systemic immunity regulated intestinal progenitor cell numbers. Since Toll is the pathway primarily responding to fungal infections in Drosophila (reviewed in Kounatidis and Ligoxygakis 2012), we attempted to reproduce the result by mimicking Toll triggering by infection. To this end, we expressed Toll10B, a constitutively active form of Toll (Shia *et al,* 2009) in *esg*-expressing cells with the GAL4/GAL80^{ts}/UAS system (*esg^{ts}>Toll10B*). This led to a significant increase of GFP positive (GFP^{+}) cells (Fig. 1C). When we expressed UAS-Toll10B and UAS-GFP with *Su(H)*-GAL4, GAL80^{ts} [*Su(H)^{ts}*, an EB-specific GAL4; Zeng et al, 2010], we also observed a significant rise in the numbers of large GFP^{+} cells (resembling EBs) in *Su(H)^{ts}>Toll10B* flies (Fig. 1C). This could be interpreted as either 1) Toll signalling creating a "roadblock" for further EB differentiation (hence the increase in GFP cells may be a "backlog" of EBs) or 2) Toll inducing division of the existing EBs to produce more of the same. However, staining with an antibody against the phosphorylated form of Histone 3 (pH3) to assay cell proliferation did not show any pH3 staining in *Su(H)^{ts}>Toll10B* guts (Fig. S1A). This indicated that the increase of GFP^{+} cells in *Su(H)^{ts}>Toll10B* flies was not a result of EB proliferation. Nevertheless, data in Fig. 1 show that

97 systemic *C. albicans* infection or constitutive Toll signalling was sufficient to increase the pool of
98 progenitor cells.

99 We next asked whether, in addition to being sufficient, Toll was also necessary for
100 controlling intestinal epithelial renewal following systemic fungal infection. We silenced Toll (using
101 an RNAi line from the VDRC collection) in progenitor cells using esg^{ts}. Development proceeded at
102 the permissive temperature (18^{o}C, GAL80 ON, GAL4 OFF, Toll RNAi OFF). Emerging day 1 adults
103 were transferred to the restrictive temperature of 30^{o}C (GAL80 OFF, GAL4 ON, Toll RNAi ON) and
104 infected with *C. albicans* 20 days later. After infection we examined the number of GFP-positive cells
105 at 36h post-infection. As a control for the RNAi mechanism we used a random line from the same
106 VDRC collection ($UAS\text{-}CG7923^{RNAi}$) that did not compromise host survival when infected with *C.*
107 *albicans* and exhibited a normal lifespan compared to its genetic background in the absence of
108 infection (our unpublished observations). The use of an endogenous gene as a control instead of an
109 inert one (e.g. RFP) ensured that we controlled for the actual triggering of the RNAi mechanism *in an*
110 *existing host gene*.
111 In control flies, we observed an increase of GFP-positive cells when comparing sterile injury
112 (PBS) with septic injury (*C. albicans*) (Fig. 2A), which was statistically significant when quantified (Fig.
113 2B). Silencing Toll prevented an increase in progenitor cells following infection since GFP-positive
114 cells after PBS injection or *C. albicans* challenge were statistically inseparable when compared (Fig.
115 2B). In contrast to controls, $esg^{ts}>Toll^{RNAi}$ flies were unable to increase ISC proliferation following
116 infection (Fig. S1B). Taken together these results indicated that Toll was also necessary for the long-
117 term renewal of the intestinal epithelium following infection. Moreover, we noted that the number
118 of GFP positive cells in $esg^{ts}>CG7923^{RNAi}$ flies was significantly higher than in $esg^{ts}>Toll^{RNAi}$ flies
119 after PBS treatment, raising the possibility that the intestines of $esg^{ts}>Toll^{RNAi}$ had less progenitor
120 cells in 20-day old adult guts even in the absence of infection (Fig. 2B).

To test long-term renewal of the intestinal epithelium in the absence of infection, we assayed guts from 6-day old and 20-day old *esg^{ts}>Toll^{RNAi}* flies and compared them to chronologically age-matched *esg^{ts}>CG7923^{RNAi}* controls. When comparing 6-day old and 20-day old flies, we found that at 20 days the shape of GFP positive progenitor cells in guts of *esg^{ts}>Toll^{RNAi}* adults was significantly altered compared to *esg^{ts}>CG7923^{RNAi}*, with cells becoming smaller and more rounded (Fig. 3A). They were also significantly reduced in numbers (Fig. 3B), with the tissue becoming extremely fragile to handle. Moreover, cultivable intestinal microbiota was significantly lower at 20-days as measured by Colony Forming Units (CFUs) (Fig. 3C). The same effect on cell numbers and cell shape in 20-day old flies was also observed when Toll was silenced in EBs [*Su(H)^{ts}>Toll^{RNAi}*] (Fig. S2).

In the absence of infection, 20-day old flies mutant for the upstream-most Toll pathway component namely, *PGRP-SA^{seml}* (Michel *et al*, 2001) showed a reduction in ISC proliferation with fewer ISCs dividing to EBs (Fig 4A). The latter were marked with an antibody against anti-hrp (Han *et al,* 2015; O'Brien *et al,* 2011). Moreover, PGRP-SA-deficient flies exhibited a significant reduction in the numbers of progenitor cells in general, and ISCs in particular (Fig. 4B). This was also reflected in the very low ISC proliferation seen in *PGRP-SA^{seml}* mutants compared to controls (Fig. S3). In addition, *spz* mutant flies had significantly reduced ECs (Fig. S4). Expression of Toll10B in *PGRP-SA^{seml}* progenitor cells was able to reconstitute progenitor cells in the anterior midgut (Fig. S5A) with numbers statistically indistinguishable from yw, the genetic background of *PGRP-SA^{seml}* (Fig. S5B). Moreover, 20-day old PGRP-SA and DIF mutants showed a reduction in intestinal microbiota when total intestinal 16S rRNA genes were semi-quantified (Fig. S6), as well as significantly reduced lifespan of both male and female flies (Fig. S7). Taken together, these results showed that Toll was both necessary and sufficient for regulating the long-term regeneration potential of the intestine after an immune challenge but also in the absence of infection.

Microbiota reduction pointed towards a metabolic shift in the gut that was unable to sustain the normal density of bacterial populations in the absence of PGRP-SA/Toll signalling. The *Drosophila* homologue of 4E-BP has been shown to be activated by infections that trigger Toll signalling and has NF-κB binding sites in its promoter (Bernal and Kimbrell, 2000). Such infections include *C. albicans* and 4E-BP null mutants are susceptible to this particular immune challenge (Levitin et al, 2007). Induction of 4E-BP activity can shift the balance towards translation of uncapped mRNAs including those of AMPs (Kang *et al,* 2017) and decelerate fat metabolism (Teleman *et al,* 2005). Indeed, *C. albicans* infection of 20-day old flies induced a 4E-BP transcription reporter construct (Bernal and Kimbrell 2000) in ECs but not in progenitor cells (Fig 5A). This induction was significantly higher than injection of sterile PBS or the non-infected control (homeostasis) (Fig. 5B). 4E-BP transcriptional induction was also observed following *Staphylococcus aureus* (*S. aureus*) infection again in ECs (Fig. 6A). After immune challenge with *S. aureus*, the number of GFP+ marked progenitors were significantly increased as was transcription of 4E-BP (Fig. 6B). Importantly, Toll10B expression in progenitor cells emulated the above as it resulted also in the transcriptional upregulation of 4E-BP in ECs in a manner comparable to *C. albicans* as well as *S. aureus* infection (Fig. 7A). This increase was significantly higher than the non-infected control (Fig. 7B).

Increase of 4E-BP transcription had an effect on fat metabolism as reported previously (Teleman *et al*, 2005). 48h after *C. albicans* infection, 20-day old control flies had elevated fat levels when normalised to total body protein (Fig. 8). This increase became more prominent when considering intestinal-only triglycerides (TGs) (Fig. S8). This indicated that systemic infection in *Drosophila* adults resulted in increased intestinal accumulation of TGs and increased systemic levels of fat. Infection of 4E-BP null mutants or flies with silenced 4E-BP in ECs through the *NP1-GAL4, GAL80^{ts}* (*NP1^{ts}>4E-BP*) configuration did not produce this phenotype (Fig. 8, Fig. S8). Overexpression of Toll10B in progenitor cells had a similar effect as *C. albicans* infection but this was suppressed in a 4E-BP null genetic background indicating that fat levels were controlled by 4E-BP (Fig. 8, Fig. S8). In

the absence of infection, loss of Toll signalling (*PGRP-SA^{seml}* mutants) resulted in significantly reduced fat levels in 20-day but not in 5-day old flies (Fig. 9). The latter had the same levels of fat as the controls (Fig. 9). Reduction of fat was accompanied by a reduction in intestinal CFUs (Fig. S9). It has been established that TOR-mediated phosphorylation keeps 4E-BP activity suppressed (Hay and Sonenberg 2004). 20-day old PGRP-SA mutant flies with TOR-RNAi in ECs or treated with the mTOR inhibitor rapamycin restored fat quantities (Fig. 9) and CFUs (Fig. S9) to the level of the *yw* control. This suggested that loss of Toll signalling released TOR activity, which dampened 4E-BP's on lipid metabolism. When TOR activity was inhibited (pharmacologically or through RNAi) in *PGRP-SA* mutants, 4E-BP was able to put a brake on fat wasting and microbiota depletion. Indeed, treatment of PGRP-SA; 4E-BP double mutants or *PGRP-SA; NP1^{ts}>4E-BP^{RNAi}* flies with rapamycin was ineffective in restoring fat levels (Fig. 9) and intestinal CFUs (Fig. S9) indicating that 4E-BP was responsible for regulating fat levels and intestinal microbiota in ECs. As differences in food intake can modulate both lipid reserves as well as lifespan, we measured food intake during a week of observation (15 to 22-day old mated female flies) using a capillary feeding assay (CAFE assay, Ja *et al*, 2007). Food intake was statistically indistinguishable between PGRP-SA and 4E-BP single mutants or PGRP-SA; 4E-BP double mutants compared to *yw* controls (Fig. S10).

Long-term intestinal regeneration is important for preserving organ function. In mice, the presence of TLR4 has been linked to increased proliferation of ISCs (Neal et al, 2012). However, the effect of the absence of TLRs has been less clear. Our results show that following infection as well as in the absence of immune challenge loss of Toll signalling blocked long-term epithelial renewal and reduced gut microbiota. Conversely, constitutive Toll in progenitor cells increased EB numbers by increasing ISC proliferation and blocking EBs to differentiate. More work is needed to pinpoint how this mechanism operates.

Infection or constitutive Toll in progenitor cells induced 4E-BP transcription in ECs. 4E-BP has been shown to preserve fat storage under stress conditions while loss of its activity resulted in flies "burning" fat faster (Teleman et al, 2005). Toll-mediated induction of 4E-BP in ECs increased both

196 intestinal and systemic fat levels. Conversely, fat reserves were depleted when Toll was similarly
197 expressed but in a 4E-BP null genetic background or when 4E-BP was silenced in ECs.

198 Age-dependent loss of fat was also observed in the absence of infection in *PGRP-SA*^{seml}
199 mutants. Reduction of fat levels was reversed with the use of rapamycin, which targets mTORC1
200 (reviewed in Laplante and Sabatini, 2012) or by blocking mTOR by RNAi in ECs. This result suggested
201 that absence of Toll signalling elevated mTORC1 activity, which in turn dampened 4E-BP (Hay and
202 Sonenberg 2004). In keeping with this hypothesis *PGRP-SA; 4E-BP* or *PGRP-SA; NP1*^{ts}*>4E-BP*^{RNAi} flies
203 treated with rapamycin were unable to restore fat levels. This indicated that systemic fat levels were
204 under 4E-BP control in ECs downstream of Toll. The latter antagonised TOR in the regulation of fat
205 metabolism through 4E-BP.

206 It is tempting to speculate that in the absence of infection, PGRP-SA recognises parts of the
207 intestinal microbiota and as such activates the Toll pathway in progenitor cells, which in turn keeps
208 4E-BP activity in enterocytes thus preserving fat levels that are important for normal microbiota
209 population density. Indeed, we have observed that 4E-BP is important for the maintenance of
210 normal CFUs in the gut and we believe that it is the preservation of fat levels through 4E-BP that
211 mediates the maintenance of a normal microbiota population density. In this context, PGRP-SA
212 function resembles intestinal TLR-2, Myd88-mediated responses in the T-cell compartment of the
213 mouse gut (Kubinak et al, 2015). More work is needed to pinpoint, which constituent(s) of the
214 microbiota PGRP-SA may recognise and how the signal is transmitted from the progenitor cells to
215 ECs.

216 Our data support a model where systemic immunity to infection is directly linked to
217 epithelial renewal and intestinal regulation of fat levels through the evolutionary conserved Toll
218 receptor. This ties together the immune and metabolic aspects of intestinal physiology with long-
219 term epithelial and microbiota homeostasis.

220

221 **Materials and Methods:**

Fly strains. The genetic backgrounds control strains used in the experiments are yw. We incorporated the *PGRP-SA*^{seml} mutation (Michel *et al*, 2001) in *esg*^{ts}*>GAL4* (Buchon et al, 2009). We used the *spz*^{rm7} mutant (de Gregorio *et al,* 2002) and incorporated UAS-CG7923^{RNAi}, UAS-9080^{RNAi} and UAS-Toll^{RNAi} in *esg*^{ts}*>GAL4* and *Su[H]*^{ts}*>GAL4* (Zeng et al, 2010). All RNAi strains were obtained from the Vienna Stock Centre (Dietzl et al, 2007). Thor-lacZ (y',w*; p{lacW}Thor^{K13517}) and Thor^{2} was obtained from Bloomington Stock Centre IN USA (# BL 9558 and # BL 9559 respectively). For Toll constitutive expression we used UAS-Toll10B (Shia *et al,* 2009).

Infection. To infect flies, Candida albicans (C. albicans) strain was cultured in Sabouraud's glucose broth (SGB; Oxoid) for 18 hours; cells were harvested by centrifugation (3200 rpm for 5 minutes) and washed in sterile phosphate buffered saline (PBS). Washed fungal cells were again centrifuged and re-suspended in PBS to an optical density of approximately 0.95- 1.05 (Thermo Scientific NanoDrop 1000 spectrophotometer). The inoculant containing C. albicans strain was further diluted four-fold in PBS. Similarly, Staphylococcus aureus (S. aureus) NCTC8325-4 was cultured in TSB for 16 hours; cells were harvested by centrifugation (4000 rpm for 7 minutes) and washed in PBS. Cells were then centrifuged and re- suspended in PBS to an optical density of approximately 0.360 and further diluted 1000-fold in PBS for injection. Anaesthetized female flies were infected with 13.2nl of the C. albicans or S. aureus suspensions (or with PBS control), directly injected into the haemolymph through the dorsolateral region of the thorax, using a micro-injector (Drummond Scientific Nanoinject II). The number of viable yeast cells injected per fly was approximately 600, as calculated from plating homogenates of six injected flies, previously ground in SGB medium. Flies were kept at 30°C post-infection for 36 hours and then dissected.

Gut dissection and immunostaining. For gut imaging, guts from anesthetized flies were dissected in Schneider's medium and fixed for 30 min in 4% paraformaldehyde (in PBS), rinsed in PBS and then three times washed (5 min each) in wash solution, 0.1% Triton X-100 (Sigma-Aldrich) in PBS. The

248 tissue was blocked for 60 min in blocking solution (0.1% Triton X- 100, 2% BSA (Sigma-Aldrich) in PBS
249 and immunostained with primary antibodies overnight at 4°C. Samples were then washed 4 x 5 min
250 at room temperature (RT) In wash solution, incubated with secondary antibodies at RT for 2 hours,
251 washed again as before and were them stained with DAPI 1:1000 (Sigma-Aldrich). Washed guts were
252 mounted in slides with vectorshield mounting media (Vector Laboratories). The following primary
253 antibodies were used: mouse anti-β- galactosidase (40-1a-S, Developmental Studies Hybridoma
254 Bank, Iowa, USA) - 1:1000; goat anti-HRP (123-165-021, Jackson ImmunoResearch Labs. Inc.)-1:500.
255 we used donkey anti-mouse Alexa 568 antibody (Invitrogen) - 1:250 and donkey anti- goat Alexa 568
256 antibody (Invitrogen) - 1:250.
257
258 **Imaging data analysis.** Guts were imaged at 20x magnification, and all GFP marked cells (esg > Gal4)
259 co-localised with DAPI small nuclei were counted in an area of approximate size that extended
260 anteriorly from Boundary 2-3 (Buchon N et al; Cell Reports, 2013); plotted values are the number of
261 GFP marked cells per unit area or per total number of DAPI stained cells. Images were analysed using
262 ImageJ software.
263
264 **Microbiota analysis.** At the indicated age-points six female flies from each of three different vials,
265 each containing approximately 20 flies, were assayed for total microbiota load. The microbiota load
266 was determined both by plating fly extracts and by PCR amplification of the 16S ribosomal RNA gene
267 from DNA obtained from dissected guts. The remaining flies were transferred to fresh vials every
268 two days. Flies were first washed with cold ethanol (70%) and then rinsed in PBS. Flies were
269 homogenized in M.R.S broth, the extract dilutions were then spread on 229 M.R.S agar and the
270 plates were incubated at 30°C. After 48 hours, colonies were counted. For PCR assay, total DNA was
271 extracted from dissected midguts (crop and hindgut were removed) using a G hypodermic needle
272 attached to a homogenizer and using the Cells and Tissue DNA Isolation Kit (NORGEN). The 16S
273 region PCR amplification was carried out for 10ng of each DNA sample, using 50µl reaction mixtures.

The primer sequences used were AGAGTTTGATCCTGGCTCAG (16S_27_Fw) and GGTTACCTTGTTACGACTT (16S_1492_Rv). A 482bp fragment from actin was also amplified in these reactions as an internal control. The primer sequences used were CTGGACTTCGAGCAGGAGAT (Act5C3_Fw) and GGTGGCTTGGATGCTTAGAA (Act5C2_Rv). Each reaction mixture contained 0.5µM of each primer, a 200µM concentration of each deoxynucleoside triphosphate (dNTP), and 1µM Phusion Taq polymerase (New England Biolabs). The PCR conditions 236 involved an initial denaturation step at 98°C for 30 secs followed by 35 cycles of 95°C for 30 secs, 65°C for 30 sec, and 72°C for 1 min and ended with an extension step at 72°C for 5 min in a thermocycler (T100 thermal cycler, Bio-Rad). PCR samples were run in a 0.8% agarose gel. The gel was stained with ethidium bromide, visualized and digitally photographed by Alphalimager HP Gel (Alpha 240 Innotech) imaging system. The bands intensities were analysed in Image J.

Triglyceride measurement This was done as in Teleman et al, 2005. Briefly, newly hatched L1 larvae were seeded in vials as at density of 50/vial and grown at 25^{o}C to synchronise the culture. Adults at the appropriate age were processed in batches of eight for males and six for females. Only male data are presented (of note that females did not deviate from the results obtained). Samples were processed immediately in homogenisation buffer [0.05% Tween-20 and 2x protease inhibitor (Roche) in H_2O]. After centrifugation (5000 rpm, 1min) the supernatant was transferred to a new tube and span again (14000 rpm, 3mins at 4^{o}C). To measure triglycerides 80µl of the above supernatant were mixed with 1ml of the Triglyceride Reagent (Thermo-Fisher) and incubated for 10mins at 37^{o}C. Measurements were taken at OD $_{520}$ and compared with a standardization curve. To measure protein levels, 100µl of the final supernatant was combined with 700µl of H_2O and 200µl of Bio-Rad Protein Assay Reagent and incubated at room temperature for 3mins. Measurements at OD_{595} were compared with a standardization curve.

Rapamycin feeding protocol. Fly food was microwaved and Rapamycin antibiotic- or ethanol as vehicle control was added to a final concentration of 200 µM (rapamycin is soluble in EtOH, rapamycin was Sigma 37094-10MG). The mix was then added to vials in batches of 10mls. We cultured female flies of the appropriate age (20 flies per vial) in vials containing rapamycin or ethanol treated food. Food was changed every two days for two weeks. When flies reached 20 days of age we sacrificed them and performed downstream experiments (fat level measurements or CFUs).

Capillary Feeding Assay (CAFE assay) Food intake was analysed as previously described (Ja *et al*, 2007) with some modifications. 50 flies per genotype were tested. Batches of 10 flies were placed in vials with wet tissue paper at the bottom and a capillary food source containing a blue dye. Feeding was monitored for 8 hours (light ON) and 1 hour (light OFF). Feeding amount was recorded every 1 hour and the capillaries were replaced every 2 days.

Statistical analysis. Data was analysed using GraphPad Prism 6 or R. First a D' Agostino and Pearson omnibus Normality test was conducted. If the data was found to fit a normal distribution, parametric tests were used, first ANNOVA and then a Tukey's multiple comparisons test. For the Thor-LacZ count data in the cases that did not fit the normal distribution we conduct Kruskal-Wallis test for the followed by the Dunn's multiple comparisons test to clarify the significance. R was used to analyse the GFP count data, it was fitted to a generalised linear model using a quasi-Poisson regression and then

ANNOVA and Tukey's multiple comparisons tests were employed to look for significance. For qPCR gene expression data was standardized by series of sequential corrections, including log transformation, mean centring, and autoscaling (Willems et al, 2008).

Acknowledgements: We would like to thank the Vienna and Bloomington Stock Centres, as well as Bruno Lemaitre for fly stocks and the Iowa Hybridoma Bank for antibodies. This work was funded by ERC Consolidator Grant 310912 and BBSRC Responsive Mode Grant BB/P005691/1 (both to PL).

References:

Akira S and Takeda K (2004). Toll-like receptor signalling Nature Reviews Immunology 4, 499–511.

Amcheslavsky A, Jiang J, Ip YT (2009). Tissue damage-induced intestinal stem cell division in *Drosophila*. Cell Stem Cell 4, 49-61.

Bernal A, Kimbrell DA (2000). Drosophila Thor participates in host immune defence and connects a translational regulator with innate immunity. Proc Natl Acad Sci 97, 6019-6024.

Buchon N, Broderick NA, Chakrabarti S, Lemaitre B (2009). Invasive and indigenous microbiota impact intestinal stem cell activity through multiple pathways in Drosophila. Genes Dev. 23, 2333-2344.

Chang C-I, Pili-Flouri S, Herve M, Parquet C, Cheillah Y, *et al.* (2004). A *Drosophila* pattern recognition receptor contains a peptidoglycan docking groove and unusual L,D-carboxypeptidase activity. PLoS Biol. 2, E277.

Daigneault J, Klemetsaune L, Wasserman SA (2013). The IRAK homologue Pelle is the functional counterpart of the IκB kinase in the Drosophila Toll pathway PLoS ONE 8, e75150.

De Gregorio E, Spellman PT, Tzou P, Rubin GM, Lemaitre B (2002) The Toll and Imd pathways are the major regulators of the immune response in Drosophila. EMBO J, 21, 2568-2579.

Dietzl G, Chen D, Schnorrer F, Su KC, Feliner M et al (2007). A genome-wide transgenic RNAi library for conditional gene inactivation in Drosophila. Nature 448, 151-156.

Han H, Pan C, Liu C, Lv X, Yang X et al (2015). Gut-neuron interaction via Hh signalling regulates intestinal progenitor cell differentiation in Drosophila. Cell Discov 1, 15006.

Hay and Sonenberg (2004). Upstream and downstream of mTOR. Genes Dev 18, 1926-1945.

Ja WW, Carvalho GB, Mak EM, de la Rosa NN, Fang AY *et al* (2007) Prandiology of *Drosophila* and the CAFE assay. Proc Natl Acad Sci USA 104, 8253-8256.

Jia K, Chen D, Riddle DL (2004). The TOR pathway interacts with the insulin signalling pathway to regulate *C. elegans* larval development, metabolism and lifespan. Development 131, 3897-3906.

Jiang I-H, Chosa N, Kim S-H, Nam H-J, Lemaitre B et al (2006). A Spätzle-processing enzyme required for Toll signalling activation in Drosophila innate immunity. Dev Cell 10, 45-55.

Kang MJ, Vasudevan D, Kang K, Kim K, Park J-E et al (2017). 4E-BP is a target of the GCN2-ATF4 pathway during Drosophila and ageing. J Cell Biol 216, 115-119.

Kounatidis I and Ligoxygakis P (2012). Drosophila as a model system to unravel the layers of innate immunity to infection. Open Biology doi: 10.1098/rsob.120075

Koubinak JL and Round JL (2012) Toll-like receptors promote mutually beneficial commensal-host interactions. PLoS Path 8, e1002785.

Kubinak JL, Petersen C, Stephens WZ, Soto R, Bake E et al (2015) Myd88 signalling in T-cells directs IgA-mediated control of the microbiota to promote health. Cell Host & Microbe 17, 153-163.

Laplante M, Sabatini DM (2012) mTOR signalling in growth control and disease. Cell 149, 274-293.

Lemaitre B, Miguel-Aliaga I (2013). The digestive tract of Drosophila melanogaster. Annu Rev Genet. 47, 377-404.

Levitin A, Marcil A, Tettweiler G, Laforest MJ, Oberholzer U et al (2007). Drosophila melanogaster Thor and response to Candida albicans infection. Eukaryotic Cell 6, 658-663.

Marek LR, Kagan JC (2012) Phosphoinositide Binding by the Toll Adaptor dMyD88 Controls Antibacterial Responses in Drosophila Immunity, 36, 612-622

Michel T, Reichhart J-M, Hoffmann JAH, Royet J (2001). Drosophila Toll is activated by Gram-positive bacteria through a circulating peptidoglycan recognition protein. Nature 414, 756–759.

Miron M, Verdu J, Lachance PE, Birnbaum MJ, Lasko PF et al (2001). The translational inhibitor 4E-BP is an effector of PI(3)K/Akt signalling and cell growth in Drosophila. Nat Cell Biol 3, 596-601.

374 Neal MD, Sodhi CPS, Hongpeng J, Dyer M, Egan CE et al (2012) Toll-like Receptor 4 Is Expressed on
375 Intestinal Stem Cells and Regulates Their Proliferation and Apoptosis via the p53 Up-regulated
376 Modulator of Apoptosis. Journal of Biological Chemistry 287, 37296-37308.
377 O'Brien LE, Soliman SS, Li X, Bilder D (2011). Altered model of stem cell division drive adaptive
378 intestinal growth. Cell 147, 603-614.
379 Ohlstein B, Spradling A (2006). The adult Drosophila posterior midgut is maintained by pluripotent
380 stem cells. Nature 439, 470-474.
381 Ohstein B, Spradling A (2007). Multipotent Drosophila intestinal stem cells specify daughter fates by
382 differential Notch signalling. Science 315, 9880992.
383 Shia AKH, Glittenberg M, Thompson G, Weber AN, Reichhart J-M, Ligoxygakis P (2009). Toll-
384 dependent antimicrobial responses in Drosophila larval fat body require Spaetzle secreted by
385 haemocytes. J Cell Sci. 122, 4505-4515.
386 Suster ML, Seugnet L, Bate M, Sokolowski MB (2004). Refining GAL4-driven transgene expression in
387 Drosophila with a GAL80 enhancer trap. Genesis 39, 240-245.
388 Teleman AA, Chen Y-W, Cohen SM (2005) 4E-BP functions as a metabolic brake used under stress
389 conditions but not during normal growth. Genes Dev 19, 1844-1848.
390 Tettweller G, Miron M, Jenkins M, Sonenberg N, Lasko PP (2005). Starvation and oxidative stress
391 resistance in Drosophila are mediated through the eIF4E-binding protein, d4E-BP. Genes Dev 19,
392 1840-1843.
393 Weber AN, Tauszig-Delamasure S, Hoffmann JAH, Lelievre E, Gascan H et al (2003). Binding of
394 Drosophila cytokine Spaetzle to Toll is direct and established signalling. Nature Immunology 4, 794–
395 800.
396 Willems E, Leyns L, Vandesompele J (2008) Standardization of real-time PCR gene expression data
397 from independent biological replicates. Anal Biochem 379, 127-129.
398 Zeng X, Chauhan C, Hou S X (2010) Characterization of midgut stem cell and enteroblast specific
399 GAL4 lines in *Drosophila*. Genesis 48, 607-611.

400

401 **FIGURE LEGENDS**

402 **Figure 1. Intestinal progenitor cells respond to systemic *C. albicans* infection**. Focusing on an area
403 of the anterior midgut close to the border with middle midgut **(A)** we found a significant increase in
404 large GFP-positive cells (green) found in esg^{ts}GFP intestines following injection by *C. albicans* in the
405 thorax compared to sterile injury with PBS **(B)**. This was mimicked in the absence of infection or
406 injury by the expression of a constitutively active form of the Toll receptor (Toll10B) when expressed
407 in progenitor cells (*esg-Gal4*) or just in EBs [*Su(H)-Gal4*] and compared to expression of nlsGFP **(C)**.
408 This implies that the large GFP cells seen in **(B)** were EBs. All nucleic were stained with DAPI (grey). In
409 the plots, each cicle represents the counted area from a single gut; 95% confidence interval is
410 displayed (* ($p<0.05$, *** $p<0.001$, ns = non-significant).

411 **Figure 2. Silencing Toll in intestinal progenitor cells prevents their increase during systemic**
412 **infection. (A)** 36 hours following PBS injection or systemic *C. albicans* infection the number of ISCs /
413 EBs (marked with GFP, green) increases (UAS-CG7923 ^{RNAi}), but not when the function of Toll is
414 reduced (UAS-Toll^{RNAi}) specifically in these cells (esg^{ts}>Gal4) **(B)**. Systemic infection may also induce
415 enhanced clustering (yellow asterisks) and morphological changes (compare white asterisks) to the
416 ISCs / EBs, which are diminished when Toll receptor activity is reduced. All nuclei stained with DAPI
417 (grey). Each circle represents a counted area from a single gut; 95% confidence interval is displayed.

418 **Figure 3. The Toll receptor influences the long-term renewal of gut progenitor cells in the absence**
419 **of infection. (A)** RNAi knockdown of the UAS-CG7923 was randomly chosen from the VDRC
420 collection as a control for the RNAI effect. Using UAS-Toll^{RNAi} (from the same VDRC collection) the
421 Toll receptor was knocked-down specifically in ISCs and EBs (esg-ts > Gal4) of the adult gut. This led
422 to altered morphology of progenitors, where the cells generally remained round, rarely adopting the
423 characteristic elongated and irregular shape often observed with ISCs/EBs a reduction in cell number

and alters their morphology, where the cells generally remain rounded, rarely adopting the characteristic elongated and irregular shape often observed with ISCs / EBs (compare cells marked with white asterisks). **(B)** There was also a significant reduction in the numbers of progenitor cells when Toll is knocked-down [day 6 compared with day 20 - *** ($p<0.001$)]. Each dot in the graph represents a counted area from a single gut taken from 3 biological repeats **(C)** Toll knocked-down resulted in a significant reduction of cultivable intestinal microbiota (CFUs) ($p<0.001$) in 20-day old flies; 95% confidence intervals are displayed.

Figure 4. *PGRP-SA^{seml}* mutant flies have less intestinal progenitor cells. (A) In the absence of infection, ISC (HRP positive, GFP positive) divide to produce EBs (HRP negative, GFP positive). However, in 20-day old flies that were deficient for PGRP-SA this division was not observed (see also insets). **(B)** Quantification of progenitor cells and ISCs showed that these were significantly reduced (*$p<0.05$; error bars display 95% confidence intervals, guts from 4 biological repeats were analysed). GFP expression was directed by the UAS dependent mCD8GFP transgene, which marked the cell membranes of the progenitor cells including ISCs and EBs (DAPI all nuclei).

Figure 5. Systemic *C. albicans* infection activates d4E-BP (Thor) transcription in enterocytes. (A) *thor-lacZ; esg^{ts}>GFP* flies injected with *C. albicans* were sampled 36 hours post-infection and compared to non-treated (homeostasis) or those injected with PBS (sterile injury). Gut cells stained with DAPI (blue), anti-β-galactosidase (red) and anti-GFP expressing cells (marking both ISCs and EBs). Shown are representative images from the anterior midgut taken at 63x. (B). Quantification of *thor-lacZ* expression upon systemic infection. Intensity measured using ImageJ, subtraction of the background was performed for all the samples. Ten guts were analysed (approximately 50 cells analysed per gut), 95% confidence intervals displayed, *$p<0.05$, *** $p<0.001$.

Figure 6. Systemic infection of S. aureus activates d4E-BP transcription in enterocytes. (A) *thor-lacZ; esg^{ts}>GFP* flies injected with S. aureus were sampled 36 hours post-infection and compared to

448 non-treated or those injected with PBS (sterile injury). Gut cells stained with DAPI (blue), anti-β-
449 galactosidase (red) and anti-GFP expressing cells (marking both ISCs and EBs). Shown are
450 representative images from the anterior midgut taken at 63x. **(B)** Quantification of progenitor cells
451 following *S. aureus* infection indicating that systemic bacterial infection can also increase the
452 population of intestinal progenitor cells **(C)** Quantification of *thor-lacZ* expression upon systemic *S.*
453 *aureus* infection. Intensity measured using ImageJ and subtraction of the background was
454 performed for all the samples. Ten guts were analysed (approximately 50 cells analysed per gut),
455 95% confidence intervals displayed, *p<0.05, *** p<0.001.

456 **Figure 7. Toll10B expressed in progenitor cells activates d4E-BP transcription in enterocytes. (A)**
457 Flies injected with *C. albicans* were sampled 36 hours post-infection and compared to non-treated
458 (homeostasis) or those expressing Toll10B. Gut cells stained with DAPI (blue), anti-β-galactosidase
459 (red) and anti-GFP expressing cells (marking both ISCs and EBs). Shown are representative images
460 from the anterior midgut taken at 63x. Two left hand columns show *thor-lacZ* **(B)**. Quantification of
461 *thor-lacZ; esg^{ts}>GFP*; right column *thor-lacZ; esg^{ts}>GFP* flies also express Toll10B transgene. **(B)**
462 Quantification of thor-lacZ expression upon systemic infection. Intensity measured using ImageJ,
463 subtraction of the background was performed for all the samples. Ten guts were analysed
464 (approximately 50 cells analysed per gut), 95% confidence intervals displayed, *** p<0.001.

465 **Figure 8. 4E-BP regulates systemic fat levels following infection or Toll over-expression in intestinal**
466 **progenitor cells.** Following *C. albicans* infection systemic fat levels were increased (comparison
467 between *yw* and yw-*C. albicans* p<0.001). The presence of d4E-BP ensured that fat levels are not
468 "burnt" as fast during infection since Thor mutants (4E-BP-*C. albicans*) or flies with silenced 4E-BP in
469 the ECs (*NP1^{ts}>4E-BP-RNAi*) that were infected had significantly less fat (comparison between yw-*C.*
470 *albicans* and 4E-BP or NP1ts>4E-BP-RNAi p<0.001). Toll overexpression in progenitor cells through
471 *esg-GAL4* was able to increase fat levels (comparison between *yw-C. albicans* and Toll-10B is non-
472 significant but between yw and Toll-10B p<0.001). However, in a genetic background mutant for 4E-

473 BP, Toll overexpression did not have an effect (comparison between *4E-BP-C. albicans* and Toll non-
474 significant). Error bars represent standard deviation. Bars represent mean values from three
475 independent experiments.

476 **Figure 9. PGRP-SA regulates 4E-BP and fat content in an age-dependent manner.** In the absence of
477 infection, 20-day old (but not 5-day old) PGRP-SA mutants had significantly reduced fat levels
478 (comparison between 20-day old *yw* and *PGPP-SA* $p<0.001$ but non- significant when comparing 5-
479 day old flies). Lack of PGRP-SA increased mTOR activity since either treatment of *PGRP-SA* mutants
480 with rapamycin or silencing mTOR in ECs of *PGRP-SA* deficient flies brought back normal fat levels
481 (comparison between 20-day old *yw* and PGRP-SA-rapamycin or *PGRP-SA; $NP1^{ts}$>mTOR-RNAi*
482 statistically indistinguishable). This was dependent on 4E-BP however, since fat levels of PGRP-SA;
483 4E-BP double mutants or *PGRP-SA; $NP1^{ts}$>4E-BP-RNAi* were low and insensitive to rapamycin
484 (comparison between 20-day old PGRP-SA-rapamycin and PGRP-SA; 4E-BP-rapamycin or *PGRP-SA;*
485 *$NP1^{ts}$>4E-BP-RNAi* is $p<0.001$ but the latter when compared to 20-day old PGRP-SA or 20-day old 4E-
486 BP gives a non-significant comparison). This indicated that mTOR/4E-BP signalling in the gut
487 influenced systemic fat levels. Error bars represent standard deviation. Bars represent mean values
488 from three independent experiments.

489 **Figure S1. Toll signalling endorses ISC but not EB cell proliferation. (A)** Constitutive Toll signalling
490 did not induce EB proliferation. *Su(H)^{ts}>Toll10B* flies, which express the constitutively active Toll
491 receptor variant Toll10B (green channel) did not activate proliferation as shown by the lack of
492 staining for pH3 (red channel). All cells were stained with DAPI (blue channel). **(B)** Silencing Toll in
493 ISCs with a *esg^{ts}>UAS-Toll-RNAi* configuration prevented ISC proliferation 36h following *C. albicans*
494 infection (lower panel) compared to control flies (upper panel).

495 **Figure S2. Silencing expression of Toll in EBs reduces their number. (A)** RNAi knockdown of the Toll
496 receptor specifically in EBs [Su(H)-Gal4] of the adult gut leads to reduction in cell number and alters

497 their morphology, where the cells generally remain rounded, rarely adopting the characteristics
498 elongated and irregular shape often observed with ISCs/EBs (compared cells marked with white
499 asterisks). CG7923 RNAi line was randomly chosen from the VDRC library and used as an internal
500 control for the RNAi effect. EBs marked with GFP (green) and all nucleic stained with DAPI (grey) in
501 20-day old flies. **(B)** Quantification showed significant EB loss in the absence of Toll (95% confidence
502 interval is displayed).

503 **Figure S3. Proliferation of ISCs is absent from the intestinal epithelium of *PGRP-SA^{seml}* mutants.**
504 **(A)** Guts from 20-day old *ywPGRP-SA^{seml}; esg^{ts}>GFP* females were stained with anti-GFP (green
505 channel), DAPI (blue channel) and anti-pH3 (red channel). This is a representative sample from n=10.
506 **(B)** In contrast, *yw* flies were found to have a significantly higher number of ISCs proliferating
507 (compare red channels).

508 **Figure S4. Loss of *spz* results in the reduction of ECs.** Staining of *esg^{ts}>GFP; spz^{rm7}* or *esg^{ts}>GFP;*
509 *spz^{rm7}/+* with anti-GFP (to mark progenitor cells, upper panels) and DAPI (to distinguish ECs, lower
510 panels) in 20-day intestines. The homozygous *spz^{rm7}* flies exhibited significantly lower numbers of
511 ECs than heterozygous *spz^{rm7}* flies ($p<0.05$, unpaired t-test). Each dot in the graph represents the
512 average number of ECs from 15 guts as measured placing a square always the same size at a random
513 point on the surface plane of the anterior midgut epithelium.

514 **Figure S5. Constitutive expression of Toll in progenitor cells rescues ISC numbers in the absence of**
515 **PGRP-SA. (A)** Expression of Toll10B in progenitor cells (*esg^{ts}>Toll10B*) in a genetic background
516 mutant for *PGRP-SA* recovers ISCs cell numbers; ISCs are labelled in red (HRP staining) while ISCs and
517 EBs are labelled in green (GFP) in 20-day old flies. **(B)** This can be verified comparing the *yw* genetic
518 background with the *PGRP-SA^{seml}; esg^{ts}>Toll10B* flies where ISC numbers were statistically
519 indistinguishable; (** $p<0.01$).

Figure S6. Loss of Toll signalling results in loss of intestinal microbiota. (A) Semi-quantitative PCR of 16S rRNA shows an age-dependent reduction in total intestinal microbiota when comparing *yw* to *PGRP-SA*^{seml} or *Dif*^{1} but no reduction in the internal control (actin). **(B)** Quantification showed a significant reduction in the quantities of 16S.

Figure S7. Loss of PGRP-SA function reduces lifespan. Both female and male flies with a deficiency in PGRP-SA function (carrying the *seml* mutation) have a significantly reduced lifespan. Median lifespan of control *yw* females was 58 days vs. 20 days for *seml* females while median lifespan of control *yw* males was 41 days vs. 18.5 for *seml* males.

Figure S8. Toll signalling regulates intestinal triglyceride levels through the TOR/4E-BP axis. Following *C. albicans* infection, intestinal fat levels increase (comparison between yw and yw-*C. albicans* $p<0.001$). The presence of d4E-BP ensures that intestinal fat levels are not "burnt" as fast during infection since infected Thor mutants (4E-BP-*C. albicans*) or flies with silenced 4E-BP in the ECs (*NP1*^{ts}*>4E-BP-RNAi*) have significantly less fat (comparison between yw-*C. albicans* and 4E-BP or NP1ts>4E-BP-RNAi $p<0.001$). Toll overexpression in progenitor cells through *esg-GAL4* increases intestinal fat levels (comparison between *yw-C. albicans* and Toll-10B is non-significant but between yw and Toll-10B $p<0.001$). However, in a genetic background mutant for 4E-BP, Toll overexpression does not have an effect (comparison between *4E-BP-C. albicans* and Toll non- significant). Error bars represent standard deviation. Bars represent mean values from three independent experiments.

Figure S9. Toll signalling regulates intestinal microbiota levels through the TOR/4E-BP axis. 20-day old *yw* flies display significantly more intestinal CFUs than *PGRP-SA*^{seml} mutants ($p<0.01$). Loss of CFUs can be rectified by treating *PGRP-SA*^{seml} with rapamycin. However, this is dependent on 4E-BP since treatment with rapamycin of a double *PGRP-SA; 4E-BP* mutant (or flies mutant for *PGRP-SA* and with 4E-BP silenced in ECs) have CFUs at the level of *PGRP-SA*^{seml}.

Figure S10. Food intake is not influenced by lack of either PGRP-SA or/and 4E-BP function. Food consumption was measured by the CAFE method in mated females (as they had a better life expectancy in PGRP-SA mutants see Fig. S6) from day 15 to day 22 of adulthood; n=5 vials (of 10 flies each) per genotype; no comparison was statistically significant ($p>0.05$, unpaired t-test).

A

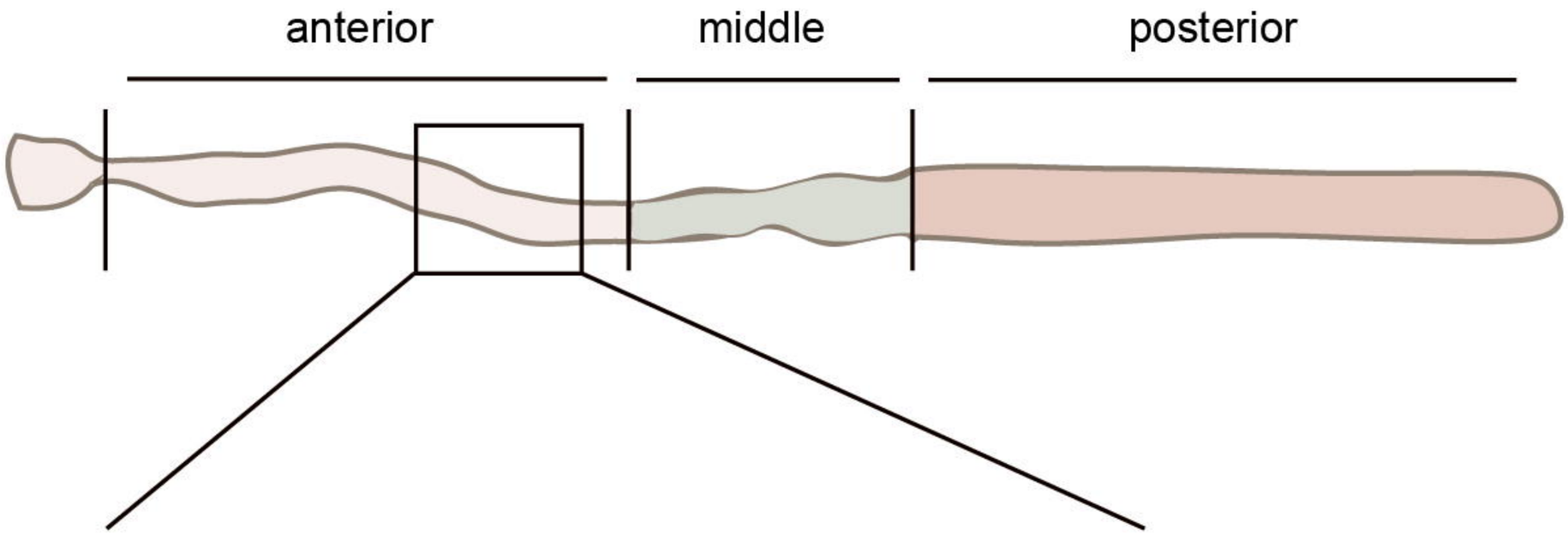

B

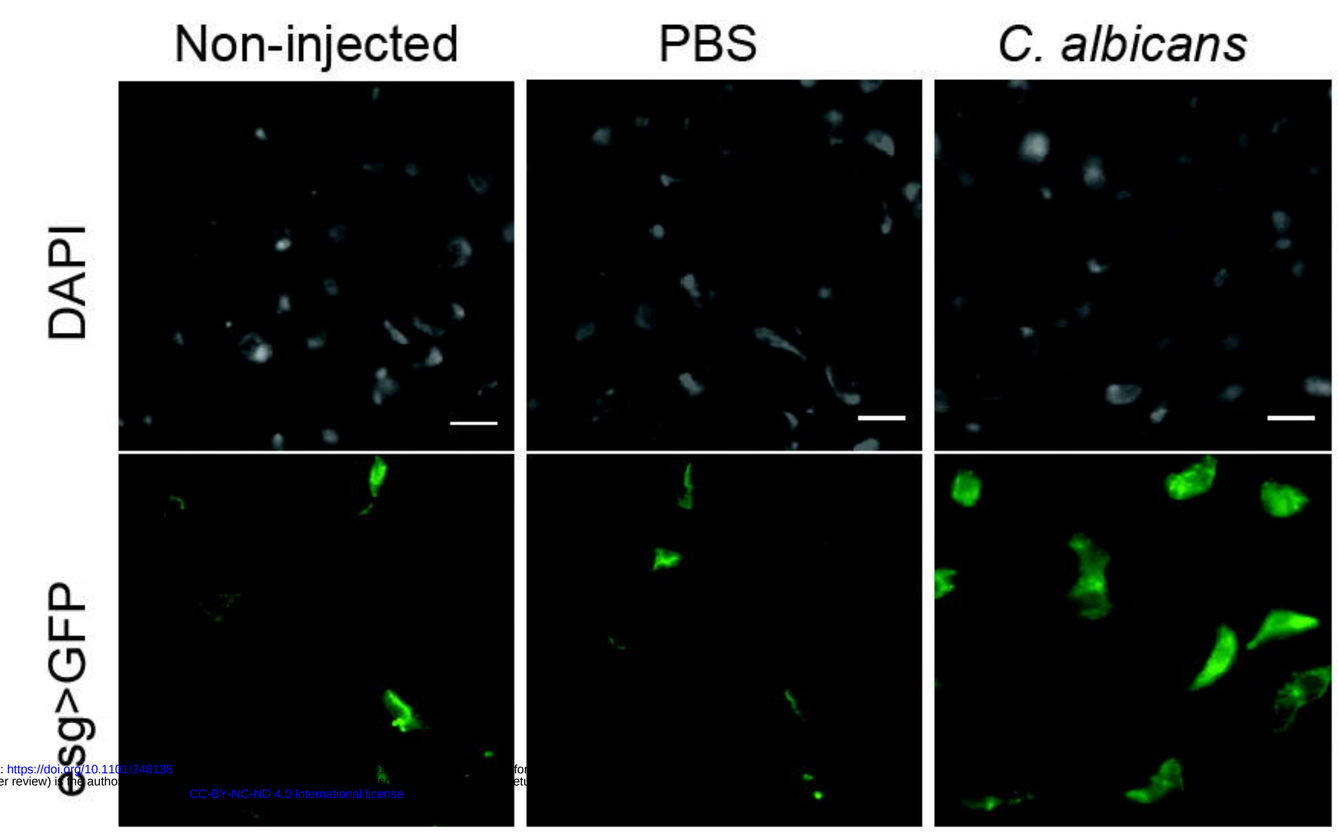

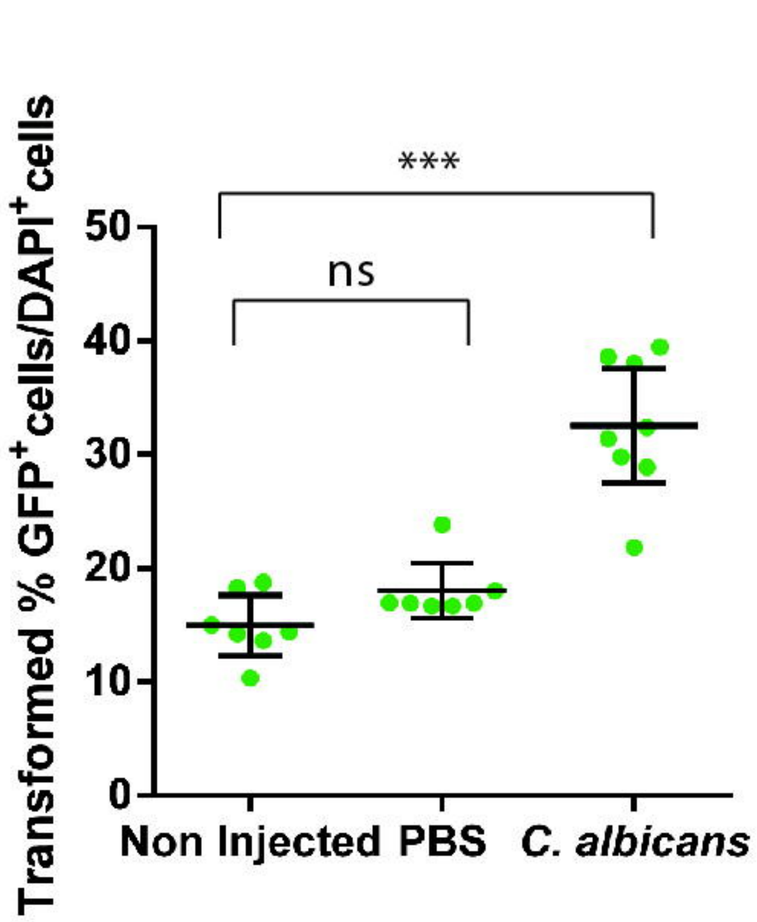

C

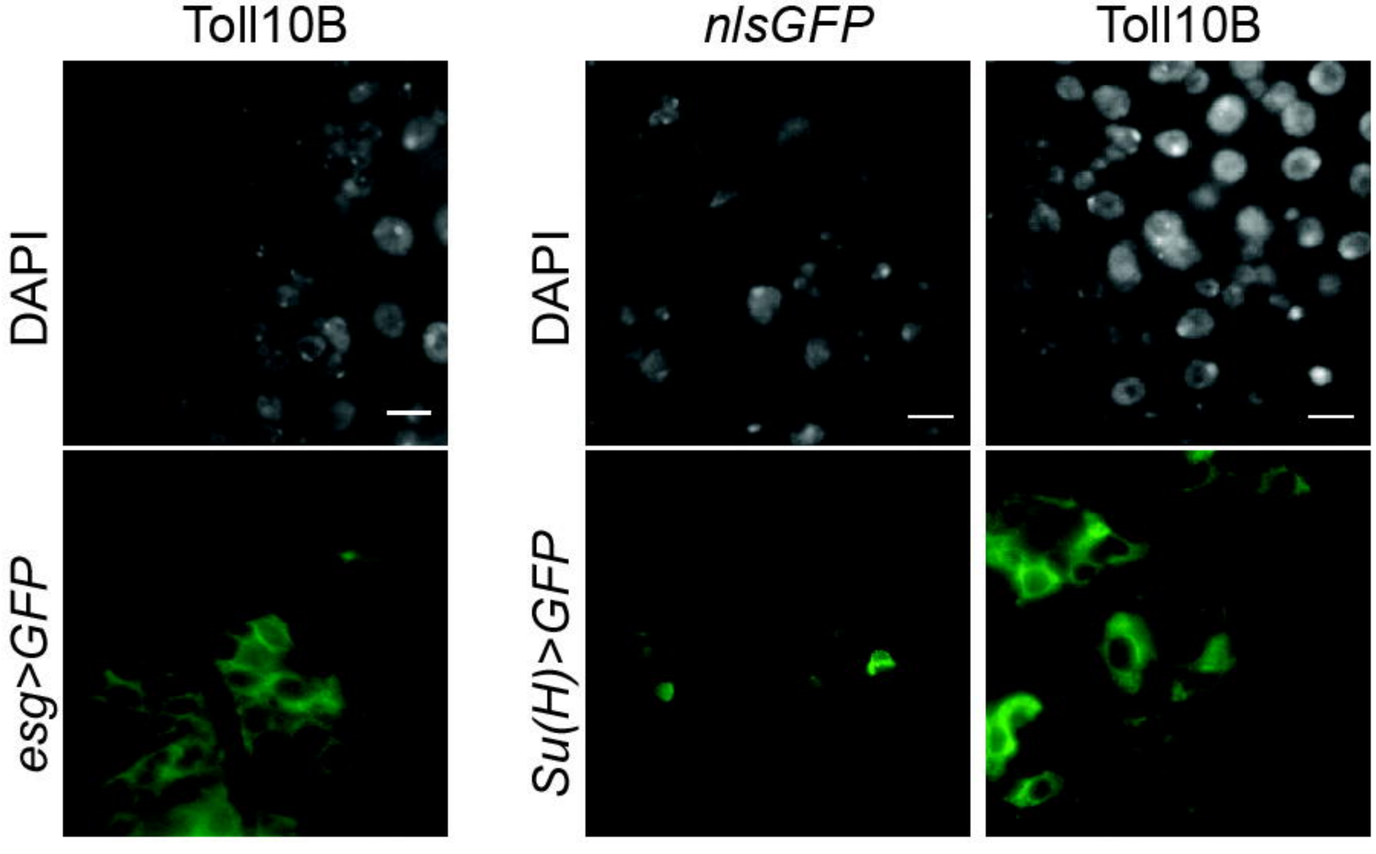

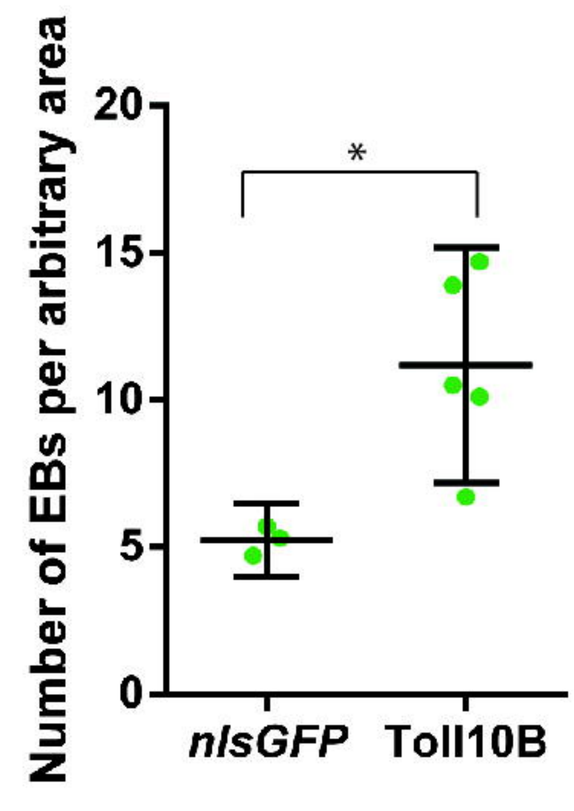

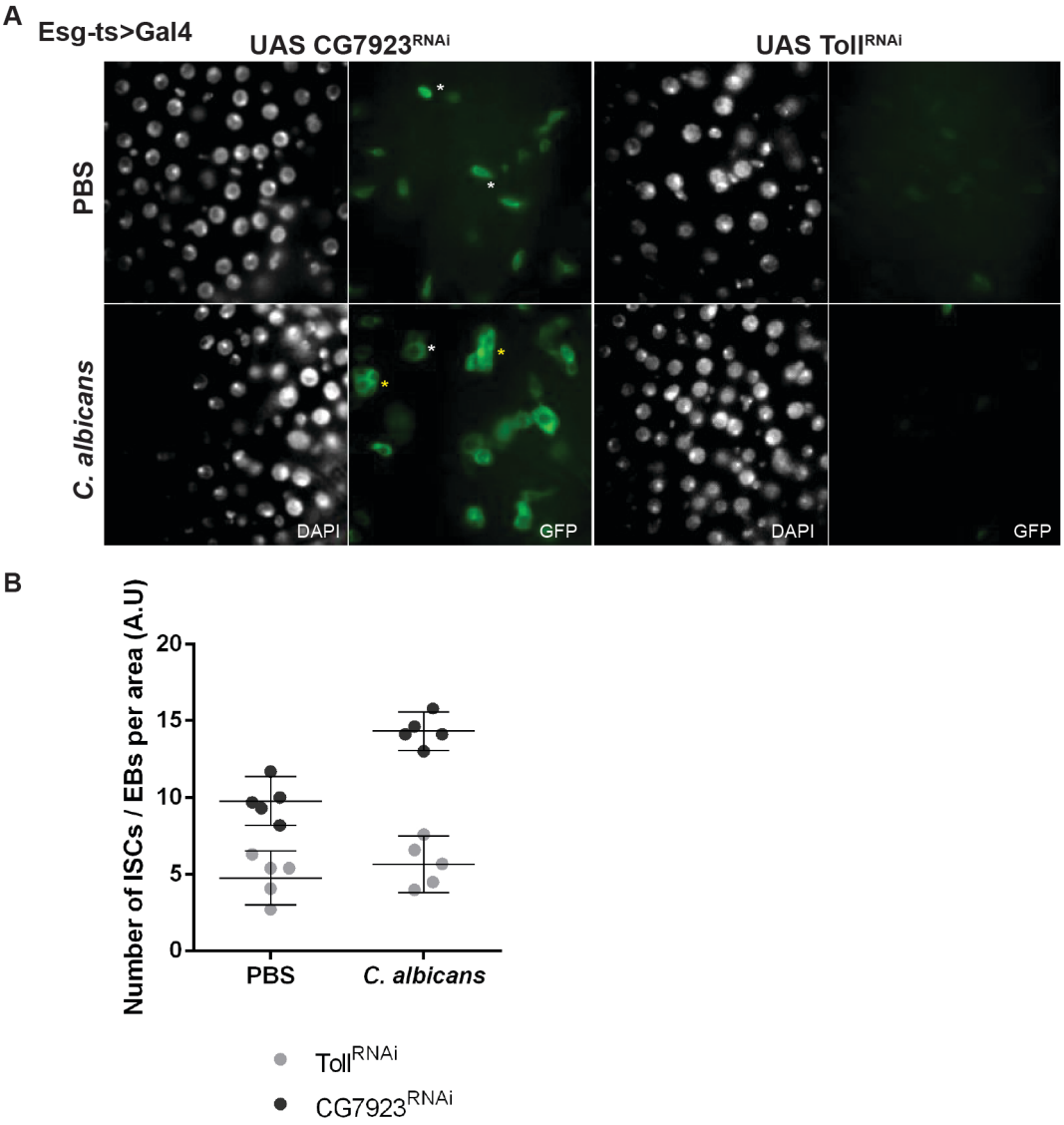

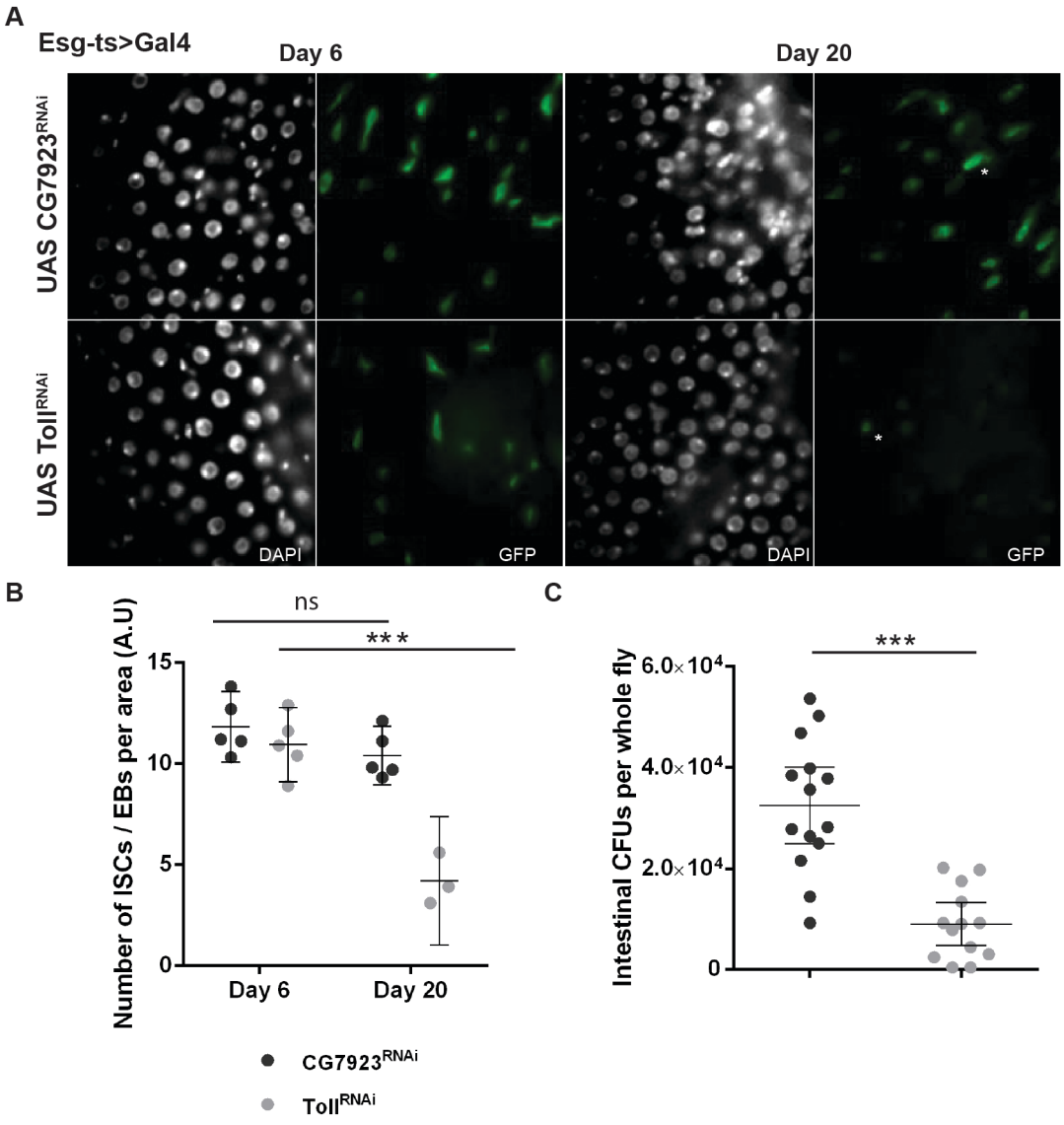

A

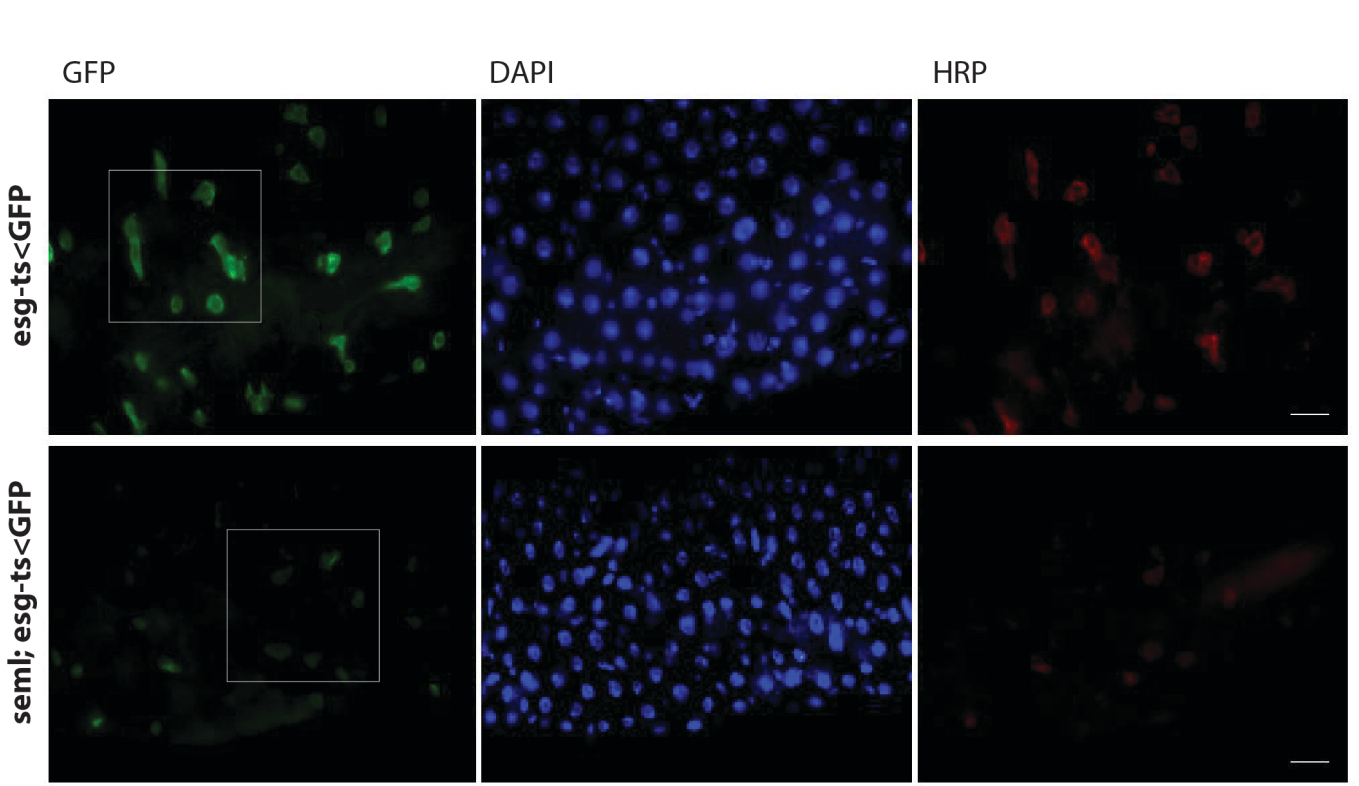

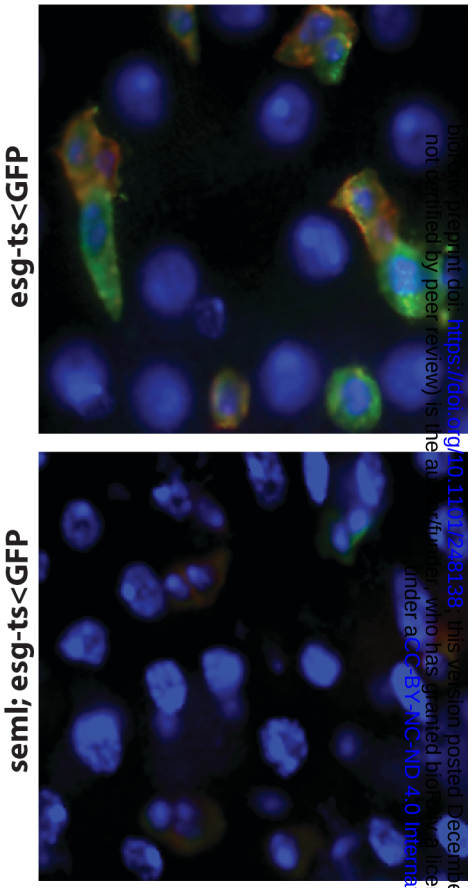

B